RSC Advances

ROYAL SOCIETY OF CHEMISTRY

www.rsc.org/advances

Journal Name

ARTICLE

Breakdown of Self-limiting Growth on Oxidized Copper Substrate: a Facile Way for Large-size High-quality Bi- and Trilayer Graphene Synthesis

Received 00th January 20xx,
Accepted 00th January 20xx

DOI: 10.1039/x0xx00000x

www.rsc.org/

Yiwei Yu, Lin Gan,* Xiaofei Wan, Tianyou Zhai*

Synthesis of large sized high-quality bi- and trilayer graphene grains in chemical vapor deposition on copper surface is still a challenge due to the self-limiting growth. In this work, we have demonstrated a facile way to break the self-limiting growth on copper by replacing the fresh copper surface with oxidized copper surface, in which the copper nanoparticles induced by oxidation take a vital role in the graphene nucleation process. As a result, high yield of bi- and trilayer graphene grains with average size of ~ 80 μm and ~ 50 μm in diameter can be easily achieved. The high quality of grains has been identified by Raman, selected area electron diffraction and electronic measurement. Moreover, the yield and distribution of bi- and trilayer grains can be tuned by the morphologies of oxidized copper substrates, namely, the distribution of copper nanoparticles, supporting the strong positive relation between copper nanoparticles and graphene nucleuses (bi- and trilayer grains).

1. Introduction

It has long been known that the properties of graphene are strongly related with its layer numbers.[1, 2] Monolayer graphene exhibited excellent electronic, mechanical and optical properties, which was supposed to compete with single-crystal silicon in semiconductor industry.[3] However, the gapless band structure of monolayer graphene[4] frustrated the efforts on logic circuit construction because shutting down the current in "off-state" is almost an impossible mission to date. Although many strategies have been employed to open a band gap in monolayer graphene, the drastic carrier mobility degradation in graphene sheet is a severe problem cannot be circumvented.[5-7] Consequently, Bernal stacking or ab-stacking bilayer graphene attracted great attention for its tunable bandgap under vertical electrical fields,[8] providing a promising chance to overcome the disadvantage of monolayer graphene in logic device. Besides, more and more researches focused on trilayer graphene have been reported in recent years for the intriguing electronic properties of trilayer graphene induced by different stacking orders, ABA and ABC.[9, 10] Currently, chemical vapor deposition (CVD) method has dominated the fabrication of various thicknesses of graphene grains as its products are of high reproducibility, high quality and acceptable yield. Nickel was once used as substrate for graphene growth; however, the drawbacks of random distribution in graphene thickness and low quality of as-grown grains [11] make it to be an unfavorite choice as a growth substrate, attributing to the high carbon solubility in nickel. Although a binary Mo-Ni alloy substrate has been proposed for graphene layer number control,[12] the rational design of such types of alloy is still under development. In opposite to nickel, copper has a very low carbon absorption capability, inducing an obvious advantage over other types of metal substrates on large sized high-quality monolayer graphene sheet synthesis, namely self-limiting growth.[13] However, limited exactly by the low solubility of carbon in copper, large sized high-quality bi- and trilayer graphene synthesis is still a challenge. For bilayer graphene synthesis, some novel synthetic strategies, in which self-limiting growth on copper was broken by extra carbon source or extreme growth condition, have been proposed and high yield ab-stacking bilayer structure can be achieved,[14, 15] although the average size of bilayer was limited in few tens of micrometer scale. In contrast, only a few works have been published on trilayer graphene synthesis to date.[16-18] Worse, either impurity adsorption in as-prepared sample or complex and time consuming fabrication process would degrade trilayer graphene properties and hamper its wide utilization.

In this work, we proposed a new strategy, as shown in **Scheme 1**, to fabricate large sized high-quality of bi- and trilayer graphene in atmospheric pressure chemical vapor deposition (APCVD), in which an oxidized copper instead of a fresh copper has been employed as growth substrate. The main difference between oxidized copper and fresh copper is

State Key Laboratory of Material Processing and Die & Mould Technology, School of Materials Science and Engineering, Huazhong University of Science and Technology (HUST), Wuhan 430074, P. R. China.
Tianyou Zhai, Email: zhaity@hust.edu.cn
Lin Gan, Email: ganlinust@hust.edu.cn
Electronic Supplementary Information (ESI) available: more optical, Raman and AFM images. See DOI: 10.1039/x0xx00000x

the surface morphologies. After oxidation treatment, a large number of copper nanoparticles would be generated on copper surface.[19, 20] Therefore during the growth process, different from conventional APCVD method, here copper nanoparticles instead of the whole copper surface work as nucleation center for graphene growth,[20] consequently, the self-limiting growth would be broken under such a nanoparticle-assisted growth environment and high yield of high-quality bi- and trilayer graphene can be easily achieved. The large size of bi- and trilayer can be attributed to the novel growth method, i.e., copper nanoparticles seeded growth method, which ensure the graphene grains more growth time than conventional growth method for its ultralow nucleation density.[21] Moreover, the density of bi- and trilayer graphene can be further modulated via the morphology of oxidized copper surface.

2. Experimental part

2.1 Copper substrate pretreatment

Copper substrate was purchased from Alfa Aesar (stock no. 13382). The copper was cut into rectangle shape of 1.8 cm × 8 cm and then polished with $FeCl_3$ regent (5g $FeCl_3$, 10 ml HCl and 100 ml DI water) for 10 – 15 s in supersonic to remove copper oxide or impurities on as-received product. Finally, using nitrogen gas gun blow-dried the copper substrate.

2.2 Oxidation of copper substrate

To achieve oxidation effect, various ways can be chosen, for example, thermal annealing the copper substrate in air on hotplate or in Ar-only (a few ppm oxygen contained) environment of CVD system. Here we adopt the latter one. 350 sccm high-purity argon gas was used to expel air in CVD system for at least 20 min, then heating the copper substrate in such an environment from room temperature to 1050 ℃ in 30 min.

2.3 Bi- and trilayer graphene synthesis

After oxidation of copper substrate, 16 sccm high-purity hydrogen was introduced into system to anneal the copper substrate for a certain time (from 0 min to 90 min). Then 16 sccm methane (500 ppm, diluted in high-purity argon) was introduced to start graphene growth. After a certain time growth (several minutes to several hours), the furnace was powered off and the system was cooling in the protection of argon and hydrogen to room temperature.

2.4 Visualization of nucleuses

The as-grown sample was thermally annealed in air on hot plate of around 300 ℃ for several minutes. At the first tens of seconds, the monolayer grains can be seen clearly in the background of oxidized copper substrate. With heating time increasing, the monolayer grains were destroyed and the nucleuses in center become visible.

2.5 Sample Characterizations and device test

The optical image was captured by Olympus DP-73; Raman spectrum was collected with LabRAM HR800 of 532 nm laser; Selected area electron diffraction (SAED) was imaged by Tecnai G2 20; AFM was scanned under semicontact mode with 512×512 resolution using a NTEGRA probe NanoLaboratory (NT-MDT, Inc.) and SPM9700. Device was fabricated on 300 nm silicon wafer and electrodes were deposited by evaporation of 10 nm Ti and 40 nm Au. The electric measurement was taken on Keithley 4200-SCS.

3 Results and discussion

3.1 Characterization of bi- and trilayer graphene

As shown in **Figure 1**, large sized bi- and trilayer graphene transferred on SiO_2 (300nm)/Si have been imaged by optical microscopy and characterized via Raman and SAED. The bilayer in figure la consists of a large sized monolayer and a smaller sized hexagonal monolayer graphene grain below it. The similar situation appears in trilayer grains (figure 1c) but a bi-layer instead of monolayer below the topmost monolayer. Single points Raman spectra have been collected to identify the layer numbers of graphene grains. As can be seen in figure 1b and 1d, the 2D and G peak, located at 2690 cm^{-1} and 1580 cm^{-1} respectively, evolves with the increase of layer numbers. In addition, the high quality of grains can be deduced from the neglectable D peak located at 1350 cm^{-1}.[22] Moreover, the stacking order of bi- and trilayer grain can also be identify by information reading from the shape of 2D peak[23] and the intensity ratio of G to 2D peak.[24] Specifically, the intensity of G/2D peak ratio increases with the layer numbers of graphene in both bi- and trilayer grains and the shape of 2D peak in trilayer grain exhibits a more symmetrical peak than in other trilayers (**Figure S1**, see supporting information). Based on above information, the stacking order in bi- and tri-layer grains can be identified to be AB and ABA modes, respectively. Besides, non-AB stacking mode of bi- and trilayer grains can also be found, as demonstrated in the SAED images (figure 1e and 1f). The two sets of diffraction pattern in figure 1e suggests that there is a certain angle between the two layers of graphene grains, in other word; it is a non-AB stacking bilayer grain.[25] Similar case occurs in the diffraction pattern of non-AB stacking trilayer grain shown in figure 1f (More optical images for non-AB stacking bi- and trilayer grains can be found in **Figure S2**). Further, the high quality of grains can also be deduced from the sharp spots shown in the diffraction patterns, in accord with the tiny D peak shown in Raman spectrum.

3.2 Distribution and statistic of bi- and trilayer graphene

The bi- and trilayer grains are actually the nucleation center of monolayer graphene grains, which distributed on the whole copper substrate but mainly concentrated along the periphery of copper. Here an improved visualization method[26] has been adopted to full monitor the distribution of nucleuses on copper, as can be seen in **Figure 2a**, the nucleuses become visible on copper after oxidation treatment because the monolayer graphene would be broken during the oxidation process, however, for the nucleus which has more than two

layers of graphene in general, it would maintain its morphology after oxidation. The white hexagonal or flower shape grains are nucleuses and the rest gray part is monolayer graphene sheet broken by thermal treatment, more information can be found in **Figure S3**. The size and shape of nucleuses vary with the flow rate direction, as shown in Figure 2b-d, the density of nucleuses decreases with flow rate direction, accordingly, the size of nucleuses evolves in a reverse way. The non-uniform distribution of nucleus on copper, i.e., the density of nucleus along the periphery of copper is obviously higher than density in the center, which may be attributed to the gas flow environment in quartz tube for density distribution changing with different growth recipes in this experiment (**Figure S4**), in good agreement with reported work.[27] The density of nucleuses on the whole copper has been depicted in figure 2e, suggesting the bi- and trilayer grains can be grown in a large size and large scale. Certainly, bi- and trilayer grains only take a part of those nucleuses as shown in **Figure 3a**, nucleuses with more than three layers can be also found. In an arbitrary nucleus site, all graphene layers shared the same center, suggesting that all layers is nucleated from the same seed, namely, copper nanoparticle, which would be further evidenced by AFM images later. Moreover, as depicted in figure 3b, the ratio of bi- and trilayer grains in all of nucleuses are around 35% and 38% respectively, confirming by transferring sample on silicon wafer and checking by optical microscopy and Raman spectra. The size distribution for bi- and trilayer grains can be found in figure 3c and 3d, in which the average sizes are larger than 80 μm for bilayer and 50 μm for trilayer, respectively. It is worthy to note that the final size of bi- and trilayer is strongly related to the growth condition, that is, both longer growth time and lower density of nucleuses generally induce larger sized bi- and trilayer grains. Therefore, a larger sized bi- and trilayer grains can be expected through further optimization of growth condition.

3.3 Evidence for nucleation *via* copper nanoparticles

To further control the quantities of bi- and trilayer grains, the exact mechanism of nucleation on oxidized copper substrate should be explored. Here we proposed a copper nanoparticles-assisted growth mechanism, in which the general self-limiting growth on copper is broken by the copper nanoparticles. As reported by many experimental and theoretical works, metal steps or hills are easily acting as nucleation center during graphene growth,[28, 29] mainly attributing to the catalytic activity of lattice defects in such deformations. As a result, bi- and trilayer grains, even much thicker grains, can be found in those sites. In this work, copper nanoparticles conduct in a similar way as metal steps or hills, acting as the nucleation center for graphene grains. The evidence for graphene nucleating at copper nanoparticles sites have been collected with AFM images in **Figure 4**. The copper substrate without oxidation treatment demonstrates a relative smooth surface (figure 4a), with a height fluctuation blew 10 nm (inset of figure 4a). In contrast, the copper undergone oxidation treatment shows many copper nanoparticles on surface (figure 4b), with a height around tens of nanometers (inset of figure 4b). The difference between two types of copper substrate is resulted from the oxidation treatment.[20] The nucleation center of graphene grain has been studied with AFM to further confirm the role of copper nanoparticles. Figure 4c exhibits the AFM image of graphene grains grown on oxidized copper substrate. The periodical ripple appeared in figure 4c, actually, is attributed to the deformation of graphene sheet during the cooling process in growth induced by different thermal expansion coefficients between copper and graphene.[13] In other words, the whole AFM image is collected on a continuous graphene grain. Interestingly, a clear small sized hexagonal graphene grain can be seen in the right corner of image, which is the nucleus of this continuous graphene grain. A zoom-in AFM image of this nucleus is shown in figure 4d in which a copper nanoparticle with height of around 50 nm (inset of figure 4d) is just located at the center of nucleus, evidencing the copper nanoparticles exactly acting as nucleation center for graphene growth (more evidence was shown in **Figure S5**). Obviously, there is another copper nanoparticle located beside the nucleation center but it is just an isolated nanoparticle, i.e. it doesn't nucleate the graphene grain, proving that not every nanoparticle can act as nucleation center. However, the exact requirements of nucleation for copper nanoparticles are still obscure to date. The generation of copper nanoparticles has been studied in our previous work,[20] and also supported by other reported works.[19] Generally, oxidation would cause various sized copper oxide nanowire or nanoparticles, higher degree of oxidation would induce larger sized copper nanoparticle. Moreover, high temperature annealing copper substrate in hydrogen would also influence the number and size of nanoparticles. Therefore, the density and size of copper nanoparticles on copper can be adjusted through rational design the oxidation and annealing process.[20]

3.4 Modulation on the growth of bi- and trilayer graphene

To demonstrate how the density of nucleuses grains evolves with copper substrate surface morphologies, the results on three different copper surfaces have been compared. As shown in **Figure 5**, AFM images for three different substrates have been exhibited in figure 5a (polished, 5 min annealing), figure 5c (polished, 90 min annealing) and figure 5e (unpolished, 5 min annealing). Corresponding nanoparticle statistic data for size distribution have been laid out just beside the AFM images. Here we adopted 20 nm as a line to divide all nanoparticles into two parts because of only a certain part of nanoparticle taking role in graphene nucleation.[20] The total amount of copper nanoparticles, from 5 min annealing sample to 90 min annealing sample, is increasing drastically, however, the number of nanoparticles larger than 20 nm actually is decreasing. As a result, the density of monolayer grains is decreasing with the increase of annealing time, in consistent with our previous work.[20] However, for the nucleuses in monolayer grains, the density of nucleuses is much higher than that of monolayer grains, suggesting the nucleation rule for nucleuses in monolayer grains is different. As depicted in the

pie pictures, the total number of nanoparticles in 90 min annealed copper is much larger than that in 5 min annealed copper. Interestingly, the big difference seems not induce a notable difference in the nucleuses shown in figure 5b and 5d, confirming that not all of nanoparticles taking roles in the nucleuses in monolayer grains. In fact, the nanoparticle indeed strongly related with the nucleation process, supported by the figure 5e and 5f in which a much lower nanoparticles density and corresponding an obvious lower density of nucleuses can be clearly seen. The copper substrate in figure 5e is unpolished and used as as-received, that is, the surface of copper is much tighter than the polished sample (**Figure S6**), resulting in a much smaller specific surface area exposed to oxygen during the oxidation treatment, thus, the density of nanoparticle induced by oxidation would be much lower. Therefore, we conclude that the number of nanoparticles have a positive relation to the final density of nucleuses in monolayer grains. Based on this, we could modulate the final size and density of nucleuses through rational design the surface morphologies of oxidized copper substrates.

3.5 Electronic properties

Bilayer grain based field effect transistor (FET) has been fabricated to evidence the high quality of few layer grains synthesized by this method. The configuration of FET device was illustrated by a depicted image in **Figure 6a**. The whole device is fabricated on 300 nm SiO_2/Si wafer via E-beam lithography. Before electronic measurement, the device has been annealed in vacuum system for improving the contact of electrode and graphene. According to our electronic measurement shown in figure 6b, the carrier mobility in bilayer grains is calculated to be ~ 3500 $cm^2/v{\cdot}s$ at room temperature, which is comparable with exfoliated bilayer graphene in reported work.[30] The high carrier mobility evidences that the oxidized copper substrate would not degrade the properties of graphene, in consistent to the reported work.[31]

4. Conclusions

We demonstrated here a new facile method to synthesize large sized high-quality bi- and trilayer graphene grains, in which oxidized copper replaced fresh copper as growth substrate in an APCVD system. Different from conventional growth method where the whole copper substrate working as nucleation center, in this work, copper nanoparticles induced by oxidation, act as nucleation center to break the self-limiting growth in conventional growth method and modulate the density of graphene nucleuses, thus the final density of bi- and trilayer grains can be simply adjusted by different distributions of copper nanoparticles. Bi- and trilayer graphene grains of high quality has been evidenced by Raman spectra, SAED and electronic measurement, which take more than 70% in the whole few layers structures and has an average size of 80 μm for bilayer and 50 μm for trilayer grains. In short, using oxidized copper as growth substrate is a simple and effective way to fabricate large-size and high-quality bi- and trilayer graphene grains, including AB and non-AB stacking modes, which may benefit to the research of electronics and optoelectronics fields.

Acknowledgements

This work was supported by National Nature Science Foundation of China (21322106, 51472097), and Ministry of Science and Technology of China (2015CB932600). Here we also want to thank the technical support from Analytical and Testing center in Huazhong University of Science and Technology.

References

1 P. Wallace, *Phys. Rev.,* 1947, **71**, 622.
2 J. Slonczewski and P. Weiss, *Phys. Rev.,* 1958, **109**, 272.
3 K. Kim, J. Y. Choi, T. Kim, S. H. Cho and H. J. Chung, *Nature,* 2011, **479**, 338.
4 A. K. Geim and K. S. Novoselov, *Nat. Mater.,* 2007, **6**, 183.
5 X. Li, X. Wang, L. Zhang, S. Lee and H. Dai, *Science,* 2008, **319**, 1229.
6 D. C. Elias, R. R. Nair, T. M. Mohiuddin, S. V. Morozov, P. Blake, M. P. Halsall, A. C. Ferrari, D. W. Boukhvalov, M. I. Katsnelson, A. K. Geim and K. S. Novoselov, *Science,* 2009, **323**, 610.
7 J. Bai, X. Zhong, S. Jiang, Y. Huang and X. Duan, *Nat. Nanotechnol.,* 2010, **5**, 190.
8 Y. Zhang, T. T. Tang, C. Girit, Z. Hao, M. C. Martin, A. Zettl, M. F. Crommie, Y. R. Shen and F. Wang, *Nature,* 2009, **459**, 820.
9 M. Koshino and E. McCann, *Phys. Rev. B,* 2009, **79,** 125443.
10 F. Zhang, B. Sahu, H. K. Min and A. H. MacDonald, *Phys. Rev. B,* 2010, **82,** 035409.
11 A. Reina, X. Jia, J. Ho, D. Nezich, H. Son, V. Bulovic, M. S. Dresselhaus and J. Kong, *Nano Lett.,* 2009, **9**, 30.
12 B. Dai, L. Fu, Z. Zou, M. Wang, H. Xu, S. Wang and Z. Liu, *Nat. Commun.,* 2011, **2**, 522.
13 X. Li, W. Cai, J. An, S. Kim, J. Nah, D. Yang, R. Piner, A. Velamakanni, I. Jung, E. Tutuc, S. K. Banerjee, L. Colombo and R. S. Ruoff, *Science,* 2009, **324**, 1312.
14 K. Yan, H. Peng, Y. Zhou, H. Li and Z. Liu, *Nano Lett.,* 2011, **11**, 1106.
15 L. Liu, H. Zhou, R. Cheng, W. J. Yu, Y. Liu, Y. Chen, J. Shaw, X. Zhong, Y. Huang and X. Duan, *ACS Nano,* 2012, **6**, 8241.
16 R. V. Salvatierra, S. H. Domingues, M. M. Oliveira and A. J. G. Zarbin, *Carbon,* 2013, **57**, 410.
17 Z. Yan, Y. Liu, L. Ju, Z. Peng, J. Lin, G. Wang, H. Zhou, C. Xiang, E. L. Samuel, C. Kittrell, V. I. Artyukhov, F. Wang, B. I. Yakobson and J. M. Tour, *Angew. Chem. Int. Ed.,* 2014, **53**, 1565.
18 Z. Wang, M. Shoji, K. Baba, T. Ito and H. Ogata, *Carbon,* 2014, **67**, 326.
19 X. Jiang, T. Herricks and Y. Xia, *Nano Lett.,* 2002, **2**, 1333.
20 L. Gan and Z. Luo, *ACS Nano,* 2013, **7**, 9480.

21 L. Gan, H. Zhang, R. Wu, Q. Zhang, X. Ou, Y. Ding, P. Sheng and Z. Luo, *Nanoscale,* 2015, **7**, 2391.
22 A. C. Ferrari, J. C. Meyer, V. Scardaci, C. Casiraghi, M. Lazzeri, F. Mauri, S. Piscanec, D. Jiang, K. S. Novoselov, S. Roth and A. K. Geim, *Phys. Rev. Lett.,* 2006, **97**, 187401.
23 C. H. Lui, Z. Li, Z. Chen, P. V. Klimov, L. E. Brus and T. F. Heinz, *Nano Lett.,* 2011, **11**, 164.
24 J. S. Hwang, Y. H. Lin, J. Y. Hwang, R. Chang, S. Chattopadhyay, C. J. Chen, P. Chen, H. P. Chiang, T. R. Tsai, L. C. Chen and K. H. Chen, *Nanotechnology,* 2013, **24**, 015702.
25 K. Kim, S. Coh, L. Z. Tan, W. Regan, J. M. Yuk, E. Chatterjee, M. F. Crommie, M. L. Cohen, S. G. Louie and A. Zettl, *Phys. Rev. Lett.,* 2012, **108**, 246103.
26 L. Gan, H. Zhang, R. Wu, Y. Ding, P. Sheng and Z. Luo, *RSC Adv.,* 2015, **5**, 25471.
27 C. Jia, J. Jiang, L. Gan and X. Guo, *Sci. Rep.,* 2012, **2**, 707.
28 G. H. Han, F. Gunes, J. J. Bae, E. S. Kim, S. J. Chae, H. J. Shin, J. Y. Choi, D. Pribat and Y. H. Lee, *Nano Lett.,* 2011, **11**, 4144.
29 J. Gao, J. Yip, J. Zhao, B. I. Yakobson and F. Ding, *J. Am. Chem. Soc.,* 2011, **133**, 5009.
30 K. Zou and J. Zhu, *Phys. Rev. B,* 2010, **82,** 081407.
31 Y. Hao, M. S. Bharathi, L. Wang, Y. Liu, H. Chen, S. Nie, X. Wang, H. Chou, C. Tan, B. Fallahazad, H. Ramanarayan, C. W. Magnuson, E. Tutuc, B. I. Yakobson, K. F. McCarty, Y. W. Zhang, P. Kim, J. Hone, L. Colombo and R. S. Ruoff, *Science,* 2013, **342**, 720.

Figures

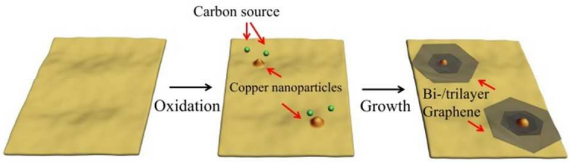

Scheme 1. Oxidized copper as substrate to synthesize bi- and trilayer graphene grains. Copper nanoparticles induced by oxidation, instead of the whole surface of copper, act as nucleation center to form bi- and trilayer graphene grains.

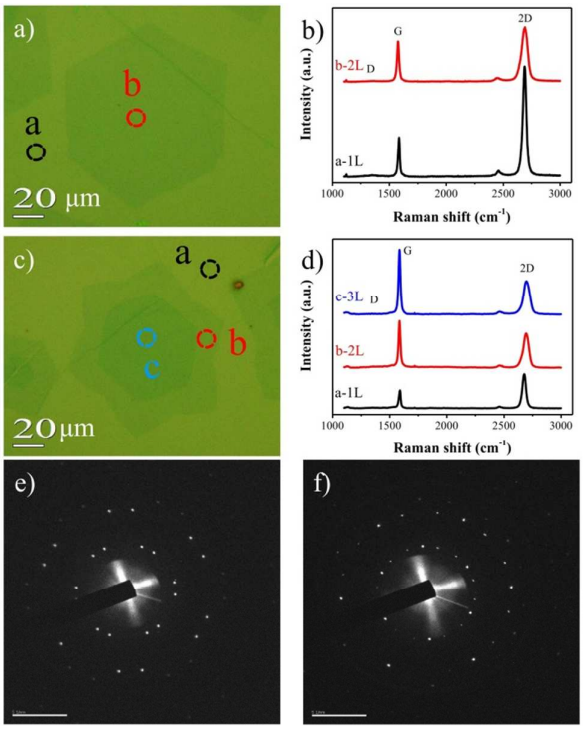

Figure 1. Bi- and trilayer graphene grains transferred on 300 nm SiO2/Si. (a) Transferred bilayer graphene grain; (b) Single points of Raman spectra at sites a and b, respectively; (c) Transferred trilayer graphene grain; (d) Single points of Raman spectra at sites a, b and c, respectively. (e,f) SAED patterns for non-AB stacking bi- and trilayer graphene grains, respectively. The scale bars are 5 1/nm in both diffraction images.

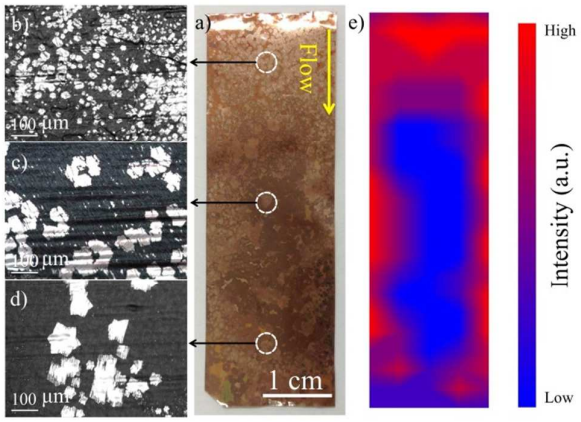

Figure 2. The distribution of graphene nucleuses on copper substrate. To visualize the nucleuses, the copper substrate was treated with high temperature thermal annealing in air. (a) Optical image for thermal treated copper substrate with graphene on surface; (b-d) Optical images for the distribution of nucleuses on different sites of copper; (e) The distribution of nucleuses shown in a 2D way according to statistic data from copper substrate.

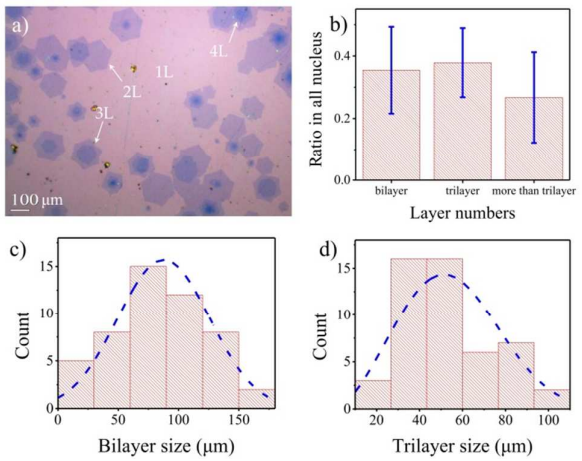

Figure 3. (a) A typical optical image for as-grown graphene sheet transferred on 300 nm SiO_2/Si. (b) The ratio of bi- and trilayer graphene grains in all nucleuses. (c,d) the statistics on the size distribution of bi- and trilayer grains, respectively.

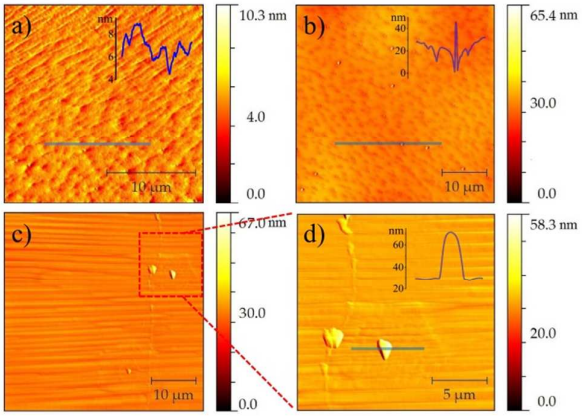

Figure 4. AFM images on copper substrates. (a) on fresh copper substrate treated with hydrogen annealing; (b) on oxidized copper substrate treated with hydrogen annealing; (c) on oxidized copper substrate with graphene; (d) the amplified image for nucleus of graphene grain, a copper nanoparticle located at the center can be clearly seen.

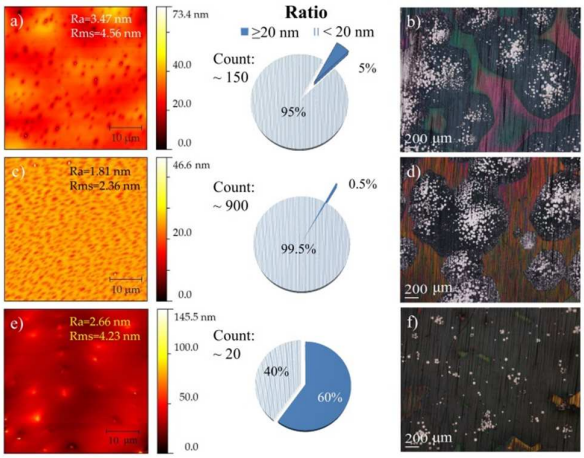

Figure 5. (a,c,e) AFM images for 5 min annealed polished copper, 90 min annealed polished copper and 5 min annealed unpolished copper, respectively. The statistics of nanoparticles distribution in size have been depicted at the right part of corresponding AFM image. The corresponding nucleuses of graphene after growth on the three types of pretreated copper substrates were shown in the optical images of (b), (d) and (f), respectively. The dark hexagons in all optical images are the oxidized monolayer graphene grain on copper and the light dots distributed in the dark hexagons are actually the nucleuses of grains.

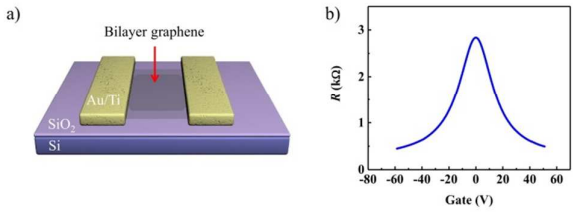

Figure 6. FET device for bilayer graphene grains synthesized via oxidized copper substrate. (a) Schematic illustration of bilayer graphene device; (b) Electronic properties of bilayer graphene measured under room temperature.